# Isotropic one-dimensional RKKY view of the magnetic phase diagrams of $U(M,M')_2X_2$ compounds

El'ad N. Caspi
*Nuclear Research Centre-Negev, P.O. Box 9001, 84190 Beer-Sheva, Israel*
*and Ben-Gurion University of the Negev, P.O. Box 653, 84105 Beer-Sheva, Israel*

Ilan Yaar and Mordechai Melamud
*Nuclear Research Centre-Negev, P.O. Box 9001, 84190 Beer-Sheva, Israel*

Hagai Shaked
*Ben-Gurion University of the Negev, P.O. Box 653, 84105 Beer-Sheva, Israel*
(Received 16 December 1999; revised manuscript received 20 March 2000)

The indirect exchange model of Ruderman, Kittel, Kasuya, and Yosida (RKKY) is used to calculate the magnetic phase diagram of $U(M,M')_2X_2$ ($M$=Ni, $M'$=Co or Cu, $X$=Si or Ge). It is found to reproduce, in a qualitative way, the measured magnetic phase diagram. Estimated values of the electron mean free path, concentration of conduction electrons, and electrical resistivity, which are deduced from these calculations, are in agreement with experimental results. Linear augmented-plane-wave calculations are also performed, and their results are in agreement with some of the RKKY results.

## I. INTRODUCTION

Compounds of the $U(M,M')_2X_2$ system ($M$=Ni, $M'$=Co or Cu, $X$=Si or Ge) crystallize predominantly in the body-centered tetragonal $ThCr_2Si_2$-type structure (I4/mmm space group). They are all paramagnetic at room temperature (RT$\sim$295 K) and undergo magnetic transitions into a variety of magnetic structures below this temperature (Fig. 1).[1–5]

The main features portrayed by these diagrams are the following: (a) Only the U atoms order magnetically with structures characteristic of ferromagnetic U basal planes stacked along the tetragonal $c$ axis according to the wave vector $\mathbf{k}=(0,0,q)$. The U-ordered moments are parallel to the $c$ axis. The (b) U magnetic structure depends strongly on the $M$ concentration; i.e., the magnetic structure highly correlates to changes in the concentration of conduction electrons, $z$,[1,2] and (c) ''oscillatory'' behavior of $T_N$ upon variations in $M$ concentration.

These unique characteristics of the $U(M,M')_2X_2$ system make it most suitable for the study of the magnetic and electronic nature of U.

In the U($5f$) atom the electronic configuration is not as well known as in the lanthanide (Ln-$4f$) atoms: the $5f$-shell radius is significantly larger than that of the $4f$ shell and its electron energies are close to the Fermi energy. Thus the total angular momentum **J** is not a ''good'' quantum number.[6] In the $U(M,M')_2X_2$ compounds, the distance between adjacent U planes is $\sim$5 Å, with two planes of nonmagnetic X atoms between them.[1–5] Obviously, a direct exchange interaction between planes of U is negligible. Thus any magnetic ordering of U along the $c$ axis should be related to an indirect exchange interaction. In this context the U $5f$ shell is expected to have a behavior similar to that of the Ln $4f$ shell. Strong evidence of this similarity was found in the $(U,Nd)Co_2Ge_2$ compounds where U was found to behave magnetically like a light Ln atom.[7]

The Ruderman-Kittel-Kasuya-Yosida (RKKY) model is an indirect exchange model, which correlates the concentration of conduction electrons, $z$, with the ground-state magnetic structures ($T$=0 K).[8–10] Also, when combining it with molecular field theory, it predicts an oscillatory behavior of $T_N$ upon changing $z$.[11] We therefore consider a one-dimensional (1D) RKKY model for the description of the magnetic interaction and structures in this system.

In the present work we reconstruct the measured magnetic phase diagrams of the $U(M,M')_2X_2$ compounds (Fig. 1) at $T$=0 K using calculations in the isotropic 1D RKKY model (see the Appendix). In order to validate some of the RKKY results, we use linear augmented-plane-wave (LAPW) calculations using the WIEN95 program.[12,13]

## II. EXPERIMENTAL RESULTS

The measured magnetic structures and the magnetic transitions temperatures of the $U(M,M')_2X_2$ compounds are summarized in two magnetic phase diagrams for $X$=Si or Ge (Fig. 1, and Refs. 4 and 5).

These measured magnetic phase diagrams are characterized by five different magnetic structures (Fig. 1). They are dominated by $\mathbf{k}=(0,0,1)$ [AF-I, corresponding to $(+\ -)$ stacking of ferromagnetic U planes] and having smaller regions of $\mathbf{k}=(0,0,2/3)$ [ferrimagnetic, $(+\ +\ -)$], $\mathbf{k}=(0,0,1/2)$ [AF-IA, $(+\ +\ -\ -)$], $\mathbf{k}=(0,0,0)$ [ferromagnetic, $(+\ +)$], and incommensurate (IC) sine-modulated structures.

One of the tests of the isotropic 1D RKKY model will be its ability to describe the observed sequence of magnetic states as a function of $M$ concentration and, in the case of the Si series, its ability to predict the existence of the unique ferrimagnetic enclave (Fig. 1).

The value of the lattice parameter ratio $c/a$ was found to

 

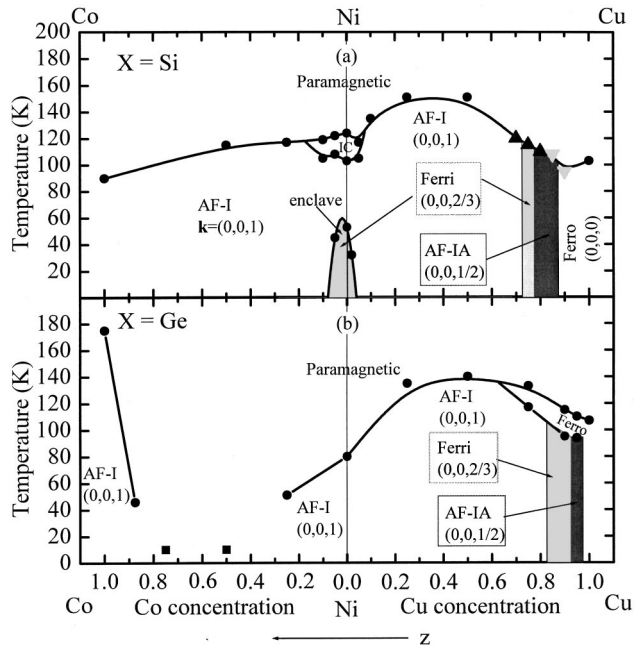


FIG. 1. The experimental magnetic phase diagram ($T_N$ vs magnetic structure) of the $U(M,M')_2X_2$ systems with $M=$Ni and $M'=$Cu or Co and (a) $X=$Si or (b) $X=$Ge. Only the U atoms order magnetically with structures characteristic of ferromagnetic U basal planes stacked along the tetragonal $c$ axis according to the wave vector $\mathbf{k}=(0,0,q)$. The U-ordered moments are parallel to $c$. Here $z$ is the number of conduction electrons per U, assumed to be proportional to the number of valence electrons of the $M$ atom. Squares indicate nonmagnetic $CaBe_2Ge_2$-type compounds.

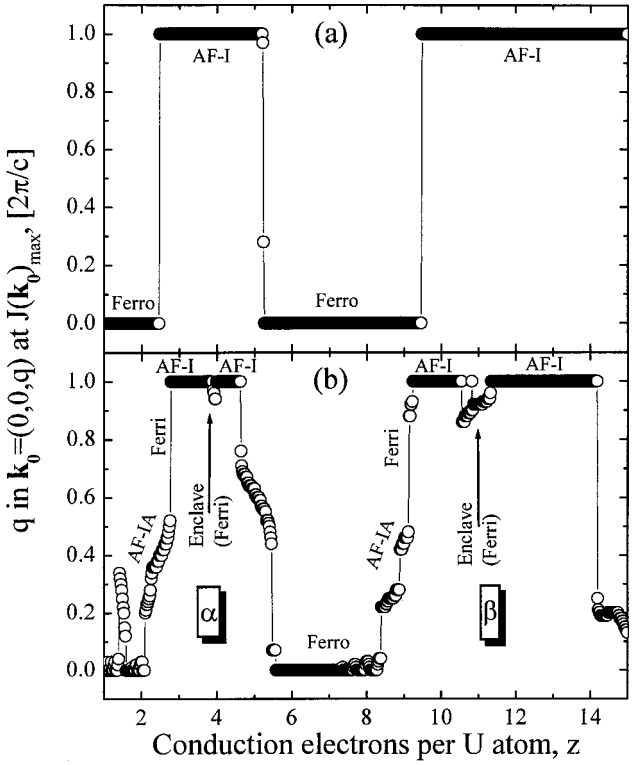


FIG. 2. Calculated magnetic phase diagrams of $UNi_2Si_2$ ($c/a=2.4037$) at 0 K showing the magnetic propagation vector vs number of conduction electrons per U atom for (a) $\lambda=1$ Å and (b) $\lambda=200$ Å. The corresponding usual notation of the main structures is shown in the diagram.

be independent of pressure in previous high-pressure (up to 0.63 GPa) neutron-diffraction measurements on $U(Ni_{1-x}Cu_x)_2Ge_2$ compounds with $x=1$ and 0.95 (i.e., isotropic linear compressibilities for both compounds).[14] Also, no change in the magnetic structures due to application of pressure of the compounds was observed. This is consistent with the isotropic 1D RKKY model, where no change in the ordered magnetic state is expected for constant $z$ and $c/a$. Moreover, the isotropy of the linear compressibilities, found in crystallographically anisotropic (uniaxial) materials, can probably be explained by a free-electron-gas-dominated compressibility. This is a reasonable result for materials in which the magnetism is mediated by conduction electrons (i.e., RKKY interaction). Following the free-electron-gas model,[15] the observed compressibilities led to $z=9.7(2)$ and 10.1(1) for $x=1$ and 0.95, respectively.[14] Thus the addition of 5% Ni (change of $x$ from 1 to 0.95) results in an increase of ~5% in $z$.

## III. RKKY CALCULATIONS

The magnetic ordering was calculated, using a PASCAL program, by summation of the Fourier transform of the RKKY exchange coefficient $J(\mathbf{k})$ over all U sites inside a sphere with a radius of 150 Å [Eq. (A4) in the Appendix]. For each of the compounds the values of $c/a$ and $\lambda$ were fixed and $q$ in $[\mathbf{k}_0=(0,0,q)]$ with minimal magnetic energy [Eq. (A3)] was calculated as a function of $z$ [Eqs. (A4)–(A6)].

*Mean free path determination.* The magnetic phase diagram of $UNi_2Si_2$ ($c/a=2.4037$ at ~10 K) in the range $z=0-20$ was calculated for various values of the conduction electron mean free path $\lambda$ in the range of 1–$\infty$. It was found that for $\lambda=1-5$ Å, only the AF-I and ferromagnetic structures are possible [Fig. 2(a)], which strongly disagrees with the experimental results [Fig. 1(a)]. For higher values of $\lambda$ the calculated magnetic phase diagram shows more complicated magnetic structures, but an enclave like range exists only for $\lambda>30$ Å near $z=11$. Another enclave appears for $\lambda=200$ Å in the vicinity of $z=4$ [Fig. 2(b)]. For 200 Å$<\lambda<\infty$ no significant changes are observed in the calculated magnetic phase diagram. Similar results were obtained in the calculations of the $UNi_2Ge_2$ compound ($c/a=2.3049$ at ~10 K, $z=0-20$). Thus the value of $\lambda=200$ Å was used for all reported calculations.

*$UNi_2Si_2$ ($c/a=2.4037$).* The calculated phase diagram ($q$ as a function of $z$ at constant $c/a$) of $UNi_2Si_2$ [Fig. 2(b)] shows two principal regions that can describe the observed sequence of magnetic transitions as a function of $M$ concentration, as well as the existence of the unique enclave [Fig. 1(a)]: The region with $z=1-5$ (region $\alpha$), which is in agreement with previous calculations,[1] and the region with $z=7-14$ [region $\beta$, expanded in Fig. 3(a)], for which no calculations were done previously. In both regions there is an enclave of $0<q<1$ between two large areas of $q=1$. In both regions, starting from the enclave (which is related to $UNi_2Si_2$) and decreasing $z$, the magnetic structure changes to AF-I ($q=1$) and then to ferromagnetic ($q=0$) passing through small regions of structures with $0<q<1$. Starting from the enclave and increasing $z$, the magnetic structure

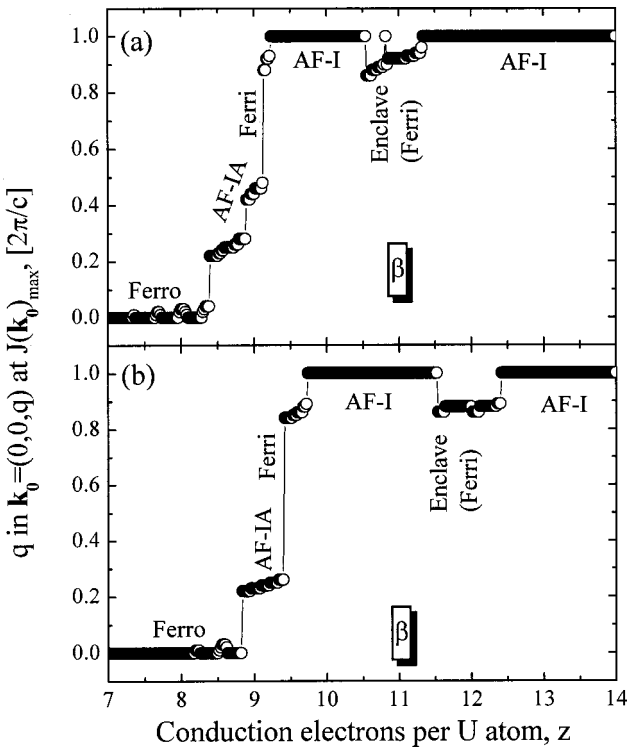


FIG. 3. Calculated magnetic phase diagrams of (a) $UNi_2Si_2$ ($c/a=2.4037$) and (b) $UNi_2Ge_2$ ($c/a=2.3049$) at 0 K and $\lambda = 200$ Å, showing the magnetic propagation vector vs number of conduction electrons per U atom. The corresponding usual notation of the main structures is shown on the diagram.

changes to AF-I. This behavior is in very good agreement with the observed phase diagram [Fig. 1(a)] for both calculated regions if the changes in $z$ are explained by substitution of Ni by Cu (decreasing $z$) or by Co (increasing $z$); see Sec. V.

*$UNi_2Ge_2$ ($c/a=2.3049$).* The calculated phase diagram of $UNi_2Ge_2$ shows in general the same features, which were obtained in the calculated phase diagram of $UNi_2Si_2$. As was previously described, the $U(M,M')_2Ge_2$ experimental magnetic phase diagram [Fig. 1(b)] lacks the unique ferrimagnetic enclave observed in the $U(M,M')_2Si_2$ experimental magnetic phase diagram [Fig. 1(a)]. Notwithstanding, a close examination of the enclave in the calculated $UNi_2Ge_2$ phase diagram is intriguing [Fig. 3(b)]. Two significant differences are detected at the corresponding region $\beta$ (Fig. 3): (a) The enclave positions for $UNi_2Si_2$ and $UNi_2Ge_2$ are at $z=11$ and 12, respectively. (b) The enclave in the $UNi_2Ge_2$ phase diagram is almost symmetric, unlike the asymmetric enclave in the $UNi_2Si_2$ phase diagram.

*The effect of $c/a$.* In order to study the effect of $c/a$ on the calculated phase diagrams of the $U(Ni_{1-x}Cu_x)_2X_2$ and $U(Co_{1-y}Ni_y)_2X_2$ systems, we calculated the magnetic structures as a function of $z$ (in the range 7–14) for the compounds for which we have experimental data (i.e., $x=0$, 0.05, 0.1, 0.25, 0.5, 0.75, 0.85, 1 and $y=0$, 0.5, 0.75, 0.9, 0.95, 1 for $X=$Si; $x=0$, 0.25, 0.5, 0.75, 0.9, 0.95, 1 and $y=0$, 0.125, 0.75, 1 for $X=$Ge). The value of $c/a$ for each of the compounds was taken from observed neutron-diffraction data at low temperatures (<10 K) and room temperatures.[2–5,14,16]

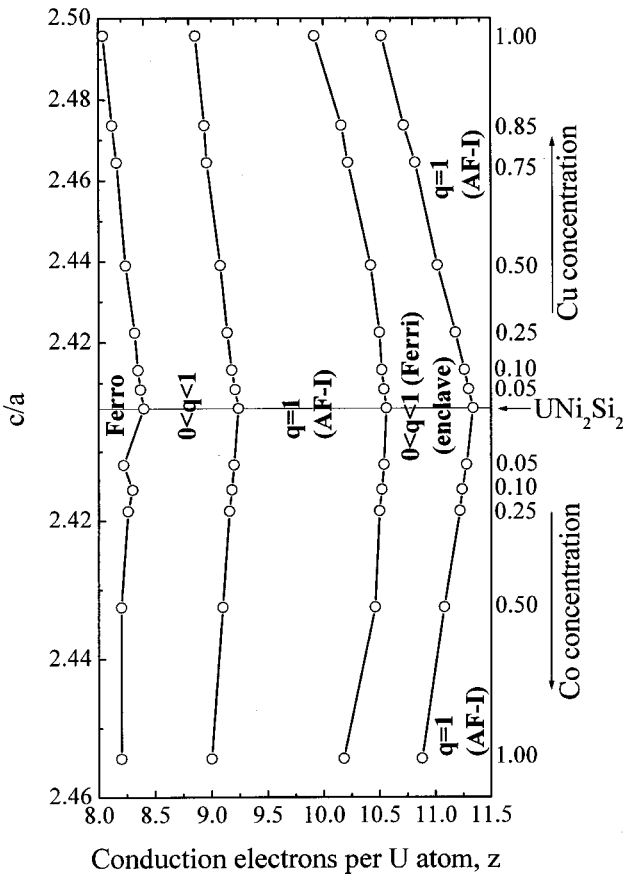


FIG. 4. Calculated magnetic structures for the $U(M,M')_2Si_2$ compounds corresponding to their lattice parameter ratio $c/a$ and number of conduction electrons per U atom, $z$.

No significant change is found in the general appearance of the calculated phase diagrams as a function of $c/a$. Nevertheless, as $c/a$ increases (i.e., as we replace Ni with either Cu or Co), the different magnetic regions (i.e., ferro, AF-I, ferri, etc.) appear for smaller $z$ values in both calculated phase diagrams (Figs. 4 and 5). The width of the ferrimagnetic enclave goes through a maximum at $UNi_2Si_2$ (Fig. 4).

## IV. LAPW CALCULATIONS

In order to validate the RKKY calculations, the electronic structure of $UM_2X_2$ compounds ($M=$Co, Ni, Cu; $X=$Si, Ge) have been investigated using the linear augmented-plane-wave (LAPW) program WIEN95.[12,13] The program takes the crystallographic structure of a compound and the electronic structures of its atoms as the input and calculates the number of conduction electrons, the partial density of states (DOS), and Fermi energy ($E_F$). The number of conduction electrons per formula unit of U, $M$, and $X$ and the total number of conduction electrons per formula unit were calculated and are 3–3.5, 0.9–1.3, 1.6–2.2, and 8–10.5, respectively. The DOS scheme of U $5f$ electrons and $M$ $3d$ electrons obtained for $UM_2Si_2$ and $UM_2Ge_2$ are depicted in Figs. 6 and 7, respectively. The DOS scheme of $UM_2Ge_2$ is in very good agreement with the results obtained previously by the augmented-spherical-wave (ASW) method.[17]

From these results it is clear that the total number of conduction electrons per formula unit for the two systems is in

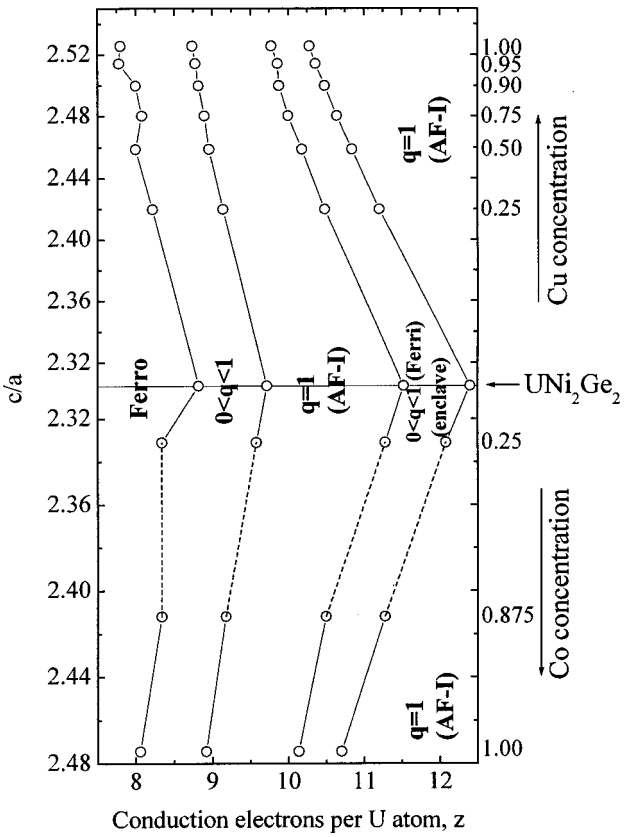


FIG. 5. Calculated magnetic structures for the $U(M,M')_2Ge_2$ compounds corresponding to their lattice parameter ratio $c/a$ and number of conduction electrons per U atom, $z$. The dashed lines corresponds to $c/a$ values for which compounds order in the $CaBe_2Ge_2$-type structure [see Fig. 1(b)].

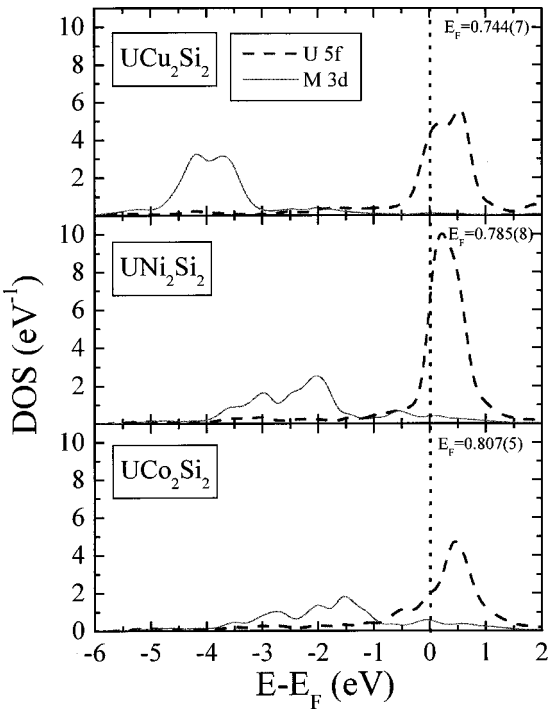


FIG. 6. Partial density of states (DOS) LAPW calculations made for $UM_2Si_2$.

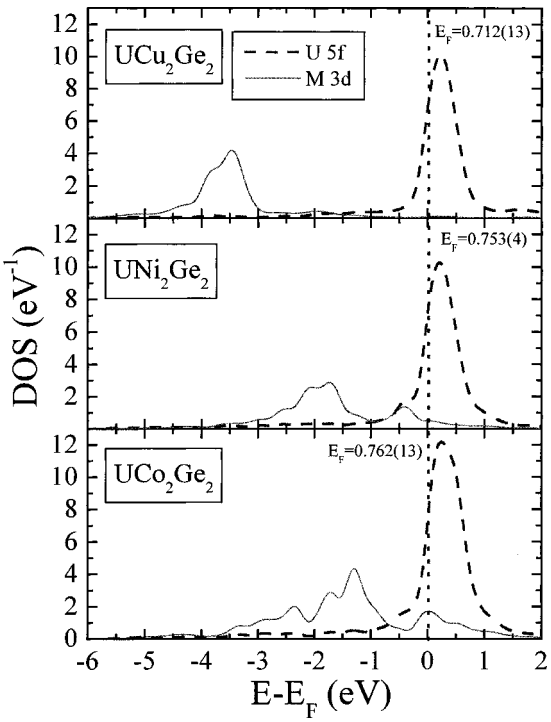


FIG. 7. Partial density of states (DOS) LAPW calculations made for $UM_2Ge_2$.

the range of 8–10.5 [region $\beta$ in the RKKY calculated phase diagrams (Fig. 2)] and not in the range of 1–4 [region $\alpha$ (Fig. 2)]. As we move from $UCo_2X_2$ to $UCu_2X_2$, one can see that for all compounds the U $5f$ band is crossed by Fermi energy, with a contribution of roughly 3 U $5f$ electrons to the conducting band (Figs. 6 and 7). At the same time, the $3d$ states of the $M$ atom move to lower energies away from $E_F$ and the probability for a $3d$ contribution to the conduction band decreases (Figs. 6 and 7). This tendency is accompanied with a decrease in $E_F$. The resulting effect of this trend should yield an almost fixed magnetic moment on the U atom and a decrease in the magnetic moment of the transition metal with an increase of its atomic number.

## V. DISCUSSION

The results of the isotropic 1D RKKY calculations are in qualitative agreement with the experimental magnetic phase diagrams. The number of conduction electrons per U atom in the $U(M,M')_2X_2$ compounds deduced from the isotropic 1D RKKY calculations could be either in the range of $z=1-5$ (region $\alpha$) or in the range of $z=7-14$ (region $\beta$) (Fig. 2). In order to resolve which of the two regions describes best the experimental phase diagram, we take into account all available experimental data. The analysis is discussed below and summarized in Table I.

LAPW calculations for these compounds result in values of $z=8-10.5$ conduction electrons per U atom (Table I). Moreover, a value of $z\sim10$ is evaluated for the $U(Ni,Cu)_2Ge_2$ compounds when applying the free-electron-gas model to the high-pressure neutron-diffraction results (Ref. 14, Table I).

One of the most obvious characteristics of the experimental magnetic phase diagrams of $U(M,M')_2X_2$ is the exis-

TABLE I. Comparison between calculated and experimental magnetic phase diagrams of the $U(M,M')_2X_2$ system. $z$ is the number of conduction electrons per U atom, $\lambda$ is their mean free path, and $\rho_\mu$ is the electrical resistivity. The calculated $\rho_\mu$ is deduced from $z$ and $\lambda$ corresponding to the enclave appearance and using the free-electron-gas model [Eq. (1)].

| | Characteristic | Calculated Region $\alpha$ | Calculated Region $\beta$ | Experimental results |
|---|---|---|---|---|
| | $z$ (RKKY) | 1–5 | 7–14 | 10[a] |
| | $z$ (LAPW) | 8.0–10.5 | | |
| | $\rho_\mu$ ($\mu\Omega$ cm) | $<4.5$ | $<16$ | 80[b] |
| | $\lambda$ (Å) | $>200$[c] | | $\sim 11$[d] |
| | | | $>30$[c] | $\sim 6$[d] |
| $X=$Si | Enclave area at Cu side vs Co side | Bigger | Smaller | Smaller |
| | AF-I area at Cu side vs Co side | Bigger | Smaller | Smaller |

[a]High-pressure neutron-diffraction results, using the free-electron-gas model (Ref. 14).

[b]Honda *et al.* at low temperature (Ref. 18).

[c]$\lambda$ at which the enclave appears.

[d]From electrical resistivity, assuming $z$ at which the enclave appears, and the free-electron-gas model.

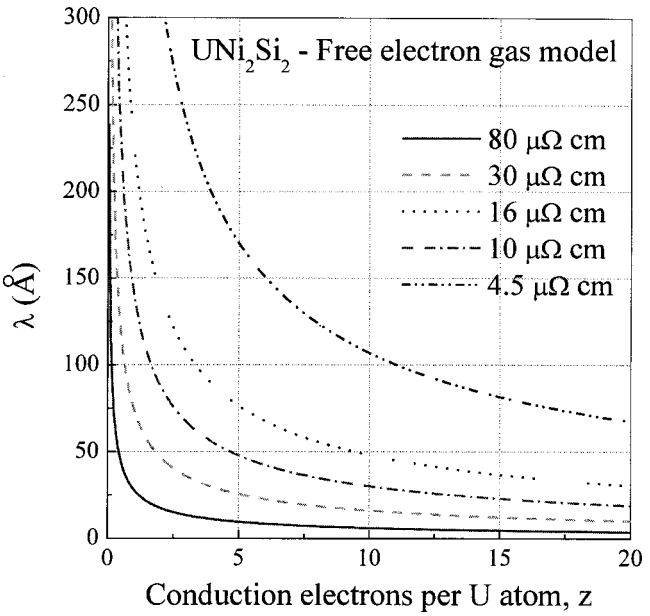


FIG. 8. Mean free path of the electrons, $\lambda$, as a function of the number of conduction electrons per U atom, $z$, for several electrical resistivities in the regime of the free-electron-gas model.

tence of regions with $0<q<1$ (Fig. 1). Whereas for magnetic structures with $q=0$ or 1 the magnetic period is one to two halves of a unit cell in the $c$ direction (5–10 Å), for structures like AF-IA $(+\ +\ -\ -)$ it is four halves of a unit cell in the $c$ direction ($\sim$20 Å). Obviously, for IC magnetic structures the magnetic period is much larger. In the RKKY model, the amplitude of the spin-density oscillations, transferring the magnetic interaction, is being damped exponentially with $e^{-R_{ij}/\lambda}$ [Eq. (A1) in the Appendix]. Therefore, it is reasonable that for $1\ \text{Å}\leqslant\lambda\leqslant 5$ Å our RKKY calculations show only the AF-I and ferromagnetic structures and that the enclave in the $z=7-14$ region does not exist below $\lambda=30$ Å and stabilizes only for $\lambda=200$ Å (Fig. 2). Thus, according to the isotropic 1D RKKY model, we may estimate that in the $U(M,M')_2X_2$ compounds the mean free path of the conduction electrons is of the order of 100 Å at low temperatures. Such a long mean free path is characteristic of the free-electron-gas model for metals at room temperature.[15] This approximation is also consistent with the results obtained in the high-pressure neutron diffraction of the $U(Ni_{1-x}Cu_x)_2Ge_2$ compounds mentioned above.[14]

Following the free-electron-gas approximation,[15] we use the relation between $\lambda$ and the electrical resistivity $\rho_\mu$,

$$\lambda=\frac{177}{\rho_\mu}\left(\frac{M_m}{z\rho}\right)^{2/3}, \tag{1}$$

where $M_m$ is the molecular mass of the material (in g/mol) and $\rho$ is the mass density of the material (in g/cm$^3$). The mean-free-path dependence on the number of conduction electrons for different electrical resistivities is depicted in Fig. 8. This figure can be used in two different ways: (1) Taking $\lambda>30$ Å for $UNi_2Si_2$, where the enclave first appears at $z\sim 10.5$ (region $\beta$), leads to an electrical resistivity of $\rho_\mu<16\ \mu\Omega$ cm (Fig. 8, Table I). On the other hand, taking $\lambda>200$ Å for $UNi_2Si_2$, where the enclave first appears at $z\sim 4$ (region $\alpha$), leads to an electrical resistivity of $\rho_\mu<4.5\ \mu\Omega$ cm (Fig. 8, Table I). (2) The experimental electrical resistivity of $UNi_2Si_2$ at low temperature is $\rho_\mu=80\ \mu\Omega$ cm.[18] Using this value, we estimate $\lambda\sim 11$ Å for region $\alpha$ and $\lambda\sim 6$ Å for region $\beta$ (Fig. 8, Table I). The total electrical resistivity, being the sum of electrical resistivities caused by different mechanisms, includes also the Kondo effect, which, if exists, raises the resistivity. Thus the existence of the Kondo effect in $UNi_2Si_2$ can explain the discrepancies between the calculated and experimental $\rho_\mu$ and $\lambda$ values (Table I). Even though both regions could explain the experimental electrical resistivity, the values corresponding to region $\beta$ are closer to reality.

Two qualitative characteristics observed in the experimental magnetic phase diagram of the $U(M,M')_2Si_2$ compounds are that (1) the enclave at the Cu side of the phase diagram is smaller than on the Co side [Fig. 1(a)]—i.e., it is asymmetric relative to $UNi_2Si_2$—and (2) the AF-I area at the Cu side of the experimental phase diagram is smaller than the AF-I area at the Co side [Fig. 1(a)]. Assuming a correlation between the number of valence electrons of the $M$ atom and conduction electrons this atom donates to the unit cell, the number of conduction electrons per U atom, $z$, is expected to decrease for a continuous substitution of Co by Ni and then of Ni by Cu. This assumption is in agreement with the LAPW results (Figs. 6 and 7) and with the high-pressure neutron-diffraction results.[14] Therefore, the Co (Cu) side in the calculated phase diagram corresponds to higher (smaller) $z$ values than the enclave's. Thus the two qualitative characteristics mentioned above are in agreement with region $\beta$ and in disagreement with region $\alpha$ [Fig. 2(b), Table I].

From the summary of the above discussion, presented in Table I, we conclude that the experimental results correspond to region $\beta$. Therefore, we find that the number of conduction electrons per U atoms in these compounds is of the order of 10 (Fig. 2).

Discrepancies between the experimental and calculated phase diagrams exist and are worth discussing, as they can lead to the refinement of the theoretical model.

The main difference between the experimental magnetic phase diagrams of $U(M,M')_2Si_2$ and $U(M,M')_2Ge_2$ is the appearance of the ferrimagnetic enclave in the former [Fig. 1(a)] and its absence in the latter [Fig. 1(b)]. This is in agreement with the RKKY and LAPW calculations, which show no ferrimagnetic enclave for the $UNi_2Ge_2$ compound. Nevertheless, the RKKY calculations suggest that there will be such an enclave when we will replace Ni with Co ($z \geqslant 11.5$). Candidate compounds for examination of this prediction, such as $U(Co_{0.5}Ni_{0.5})_2Ge_2$ and $U(Co_{0.75}Ni_{0.25})_2Ge_2$, crystallize in the $CaBe_2Ge_2$-type structure ($P4/nmm$ space group) and could not be discussed in the frame of the present work.

Discrepancies exist also with regards to the exact value of $q$ for the various structures. The $q$ value of the ferrimagnetic enclave in the experimental $U(M,M')_2Si_2$ phase diagram is 0.667, whereas the calculated value is not less than 0.85. This discrepancy may be a result of the use of an isotropic model applied to an anisotropic (tetragonal) crystal structure.

The mutual effect of $z$ and $c/a$ on the magnetic structures of the $U(M,M')_2X_2$ compounds is depicted in Figs. 4 and 5 for $U(M,M')_2Si_2$ and $U(M,M')_2Ge_2$, respectively. We find that for a given $z$, by changing $c/a$ it is not possible to reproduce the sequence of magnetic transitions found in the experimental magnetic phase diagrams (Fig. 1). Consequently, any discussion of the magnetic interactions in the $U(M,M')_2X_2$ compounds in the framework of the isotropic 1D RKKY model, requires that changes in the transition-metal concentration will correspond to changes in the number of conduction electrons per U atom, as well as the observable changes in the $c/a$ values.

## VI. CONCLUSIONS

In this work we discuss the validity of the RKKY model description of the magnetic interactions in the $U(M,M')_2X_2$ systems. From a comparison of calculations using isotropic 1D RKKY, LAPW, and free-gas-electron models, with the experimental magnetic phase diagrams, we conclude the following.

(1) The isotropic 1D RKKY model gives a qualitative description of the experimental magnetic phase diagrams of the $U(M,M')_2X_2$ systems.

(2) The magnetic ordering in these systems depends strongly on the number of conduction electrons per U atom.

(3) The estimated value of conduction electrons per U atoms in these systems is 10. This number varies in the range 8–12 as we change the transition-metal concentration in $U(M,M')_2X_2$.

(4) The estimated values of the mean free path, electrical resistivity, and number of conduction electrons per U atom, deduced from the isotropic 1D RKKY and free-electron-gas models, are in agreement with experimental results.

(5) Some discrepancies between the experimental phase diagrams and those calculated using the isotropic model were found. Future study of these discrepancies, for example, using an anisotropic 1D RKKY model, may lead to a deeper theoretical understanding of the magnetic and electronic nature of U in the compounds discussed.

## ACKNOWLEDGMENTS

The authors thank Dr. Moshe Kuznietz, and Haim Pinto for fruitful discussions, which helped shed light on some of the above problems.

## APPENDIX

*Isotropic 1D RKKY model*. The RKKY model describes the indirect exchange interaction between a pair of magnetic atoms via polarization of conduction electrons. The interaction of spin $S_i$ localized at $R_i$ with the spin density of the conduction electrons polarized by $S_j$ at $R_j$ results in an indirect interaction of $S_i$ with $S_j$ described by the Hamiltonian[19]

$$\mathcal{H}_{\mathrm{IE}} = -\frac{9\pi}{2} z^2 \frac{J_{\mathrm{sf}}^2}{E_F} \sum_{i \neq j} F(2k_F \mathbf{R}_{ij})(\mathbf{S}_i \cdot \mathbf{S}_j) e^{-R_{ij}/\lambda}, \quad \text{(A1)}$$

where

$$F(x) = \frac{-x\cos x + \sin x}{x^4}, \quad \text{(A2)}$$

$z$ is the number of conduction electrons per magnetic atom, $J_{\mathrm{sf}}$ is the exchange constant of the interaction of the localized spin with the conduction electrons, $E_F$ is the Fermi energy, and $\lambda$ is the mean free path of the conduction electrons.[20]

The interaction energy is deduced from a variational solution to the Hamiltonian in Eq. (A1) and by using the Fourier transform[18]

$$E = -N \sum_{\mathbf{k}} J(\mathbf{k}) |\mathbf{S}_{\mathbf{k}}|^2, \quad \text{(A3)}$$

where $\mathbf{S}_{\mathbf{k}}$ is the Fourier transform of $\mathbf{S}_i$, $N$ is the number of magnetic atoms, $J(\mathbf{k})$ is the Fourier transform of $J_{ij}$,[19]

$$J(\mathbf{k}) = \frac{1}{2N} \sum_{i,j} J_{ij} e^{i\mathbf{k}\cdot\mathbf{R}_{ij}}, \quad \text{(A4)}$$

and $J_{ij}$ is the RKKY exchange coefficient. Assuming a spherical Fermi surface,[19]

$$J_{ij} = \frac{9\pi}{2} J_{\mathrm{sf}}^2 \frac{z^2}{E_F} F(2k_F R_{ij}) e^{-R_{ij}/\lambda}, \quad \text{(A5)}$$

where $k_F$ is deduced from the isotropic approximation[1]

$$k_F = \frac{\pi}{a} \sqrt[3]{\frac{6z}{\pi} \frac{a}{c}}. \quad \text{(A6)}$$

Minimal magnetic energy would be achieved for maximal $J(\mathbf{k})$ [Eq. (A3)]. A PASCAL program was written, using the above equations, to calculate $J(\mathbf{k})$ for fixed values of $z$, $c/a$, and $\lambda$. The calculations yield the value of $\mathbf{k}_0$ for which $J(\mathbf{k}_0)$ is maximum. The magnetic structure with minimal energy will thus consist of ferromagnetic planes modulated with $\mathbf{k}_0$ along $c$. In this work we discuss zero-temperature calculations only.

[1] L. Chełmicki, J. Leciejewicz, and A. Zygmunt, J. Phys. Chem. Solids **46**, 529 (1985).
[2] M. Kuznietz, H. Pinto, H. Ettedgui, and M. Melamud, Phys. Rev. B **48**, 3183 (1993).
[3] M. Kuznietz, G. André, Françoise Bourée, H. Pinto, H. Ettedgui, and M. Melamud, J. Alloys Compd. **219**, 244 (1995).
[4] M. Kuznietz, H. Pinto, and M. Melamud, Physica B **223&224**, 234 (1996).
[5] M. Kuznietz, E. Caspi, H. Pinto, and M. Melamud, J. Magn. Magn. Mater. **177-181**, 51 (1998).
[6] B. R. Cooper, Q. G. Sheng, and S. P. Lim, J. Alloys Compd. **192**, 223 (1993).
[7] E. Caspi, M. Kuznietz, H. Ettedgui, H. Pinto, M. Melamud, and H. Shaked, Phys. Rev. B **57**, 449 (1998).
[8] M. A. Ruderman and C. Kittel, Phys. Rev. **96**, 99 (1954).
[9] T. Kasuya, Prog. Theor. Phys. **16**, 45 (1956).
[10] K. Yosida, Phys. Rev. **106**, 893 (1957).
[11] T. Jaworska-Gołab, M. Guillot, M. Kolenda, E. Ressouche, and A. Szytuła, J. Magn. Magn. Mater. **164**, 371 (1996).
[12] P. Blaha, K. Schwartz, and P. Herzig, Phys. Rev. Lett. **54**, 1192 (1985).
[13] P. Blaha, K. Schwartz, P. Sorantin, and S. B. Trickey, Comput. Phys. Commun. **59**, 399 (1990).
[14] E. Caspi, H. Shaked, H. Pinto, M. Melamud, Z. Hu, O. Chmaissem, S. Short, and J. D. Jorgensen, J. Alloys Compd. **271-273**, 378 (1998).
[15] N. W. Ashcroft and N. D. Mermin, *Solid State Physics* (Saunders College, Orlando, 1976), pp. 30–55.
[16] T. Endstra, Ph.D. thesis, Rijksuniversiteit te Leiden, 1992.
[17] S. F. Matar, V. Eyert, A. Mavromaras, S. Najm, B. Chevalier, and J. Etourneau, J. Magn. Magn. Mater. **174**, 219 (1997).
[18] F. Honda, G. Oomi, T. Kagayama, A. V. Andreev, V. Sechovský, L. Havela, M. I. Bartashevich, T. Goto, and A. A. Menovsky, J. Magn. Magn. Mater. **177-181**, 49 (1998).
[19] D. C. Mattis, *The Theory of Magnetism I: Statics and Dynamics* (Springer-Verlag, Berlin, 1981), pp. 229–239.
[20] J. Heeger, A. P. Klein, and P. Tu, Phys. Rev. Lett. **17**, 803 (1966).